

CHARM Facility Test Area Radiation Field

Adam Thornton

October 2015

Abstract

Specification document summarising the radiation field of the CHARM facility test area. This will act as a guide to any potential users of the facility as to what they can expect in terms of radiation, given in the form of radiation spectra information and fluence for each test position, along with general radiation maps for the test area and Montrac test location.

Contents

| | | |
|----------|---|-----------|
| 1 | Introduction | 2 |
| 2 | Facility Description | 4 |
| 2.1 | Facility Configuration | 7 |
| 2.2 | Beam Instrumentation | 9 |
| 2.2.1 | Beam Intensity Monitoring | 9 |
| 2.2.2 | Beam Position and Size Monitoring | 9 |
| 2.3 | Beam Specification | 9 |
| 2.4 | Operating Conditions | 10 |
| 3 | Radiation Field | 15 |
| 3.1 | Quantifying the Radiation Field | 15 |
| 3.2 | Metrics | 16 |
| 3.3 | Standards and Environments | 18 |
| 3.4 | FLUKA Calculations | 19 |
| 3.4.1 | FLUKA Geometry | 19 |
| 3.4.2 | Scoring | 20 |
| 4 | FLUKA Results | 21 |
| 4.1 | Overview | 21 |
| 4.2 | Copper Target without Shielding | 30 |
| 4.3 | Montrac Test Position | 33 |
| 4.4 | Uncertainties | 34 |
| 5 | Measurements and Testing | 35 |
| 5.1 | Non-shielded Positions | 35 |
| 5.2 | Shielded Positions | 35 |
| 5.3 | BLM | 35 |
| 5.4 | Montrac | 35 |
| 6 | Summary | 36 |
| A | Facility Information | 37 |

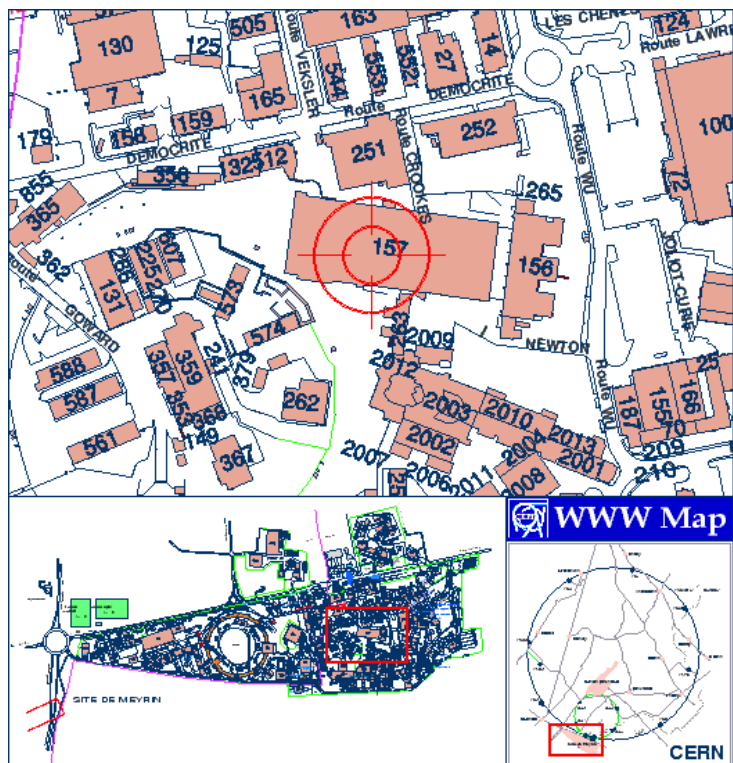
Chapter 1

Introduction

The CERN High Energy Accelerator Mixed-field (CHARM) facility is situated in the Proton Synchrotron (PS) East Area hall at the Meyrin Site of CERN in Switzerland. A map in figure 1.1 shows the location on the Meyrin site, and a 3D rendered image of the East Area hall is shown in figure 1.2. The aim of the CHARM facility is to have a flexible and dedicated place for the testing of electronics and systems in well characterised mixed-radiation fields, which can replicate a wide number of real radiation environments such as space, atmosphere, or accelerator complexes for example. To achieve this, the test area has been constructed with the sole purpose of flexibility in electronics testing.

Starting with the 24 GeV proton beam from the PS, the beam is directed along a number of beam-lines to various physics experiments. The CHARM facility is located at the end of the T8 beam-line in the PS East Area Hall. The T8 beam-line is shared with the IRRAD facility, located up-stream of CHARM. Once the beam passes through IRRAD, it enters the CHARM test area where it impinges on 1 of the 3 possible targets. Depending on the target selection, the radiation field can be varied inside the test area. Additionally, there are 4 movable shielding layers of iron and concrete inside the test area which can further alter the radiation field. Finally there are a number of dedicated test positions around the test area, which are selected based on the radiation field requirements of the user.

To understand the radiation field within the test area, dedicated FLUKA Monte Carlo calculations have been made for the various facility configurations and test positions. Using these results, one can describe the radiation spectra seen at each test position and calculate useful quantities related to electronics testing, such as the total ionising dose (TID) or 1 MeV equivalent neutron fluence in Silicon for example. A detailed list of the available information is shown in chapter 3. These values can then be used to calculate failure rates and tolerances of test equipment to be installed and used in environments where radiation is present.



Chapter 2

Facility Description

The CHARM facility consists of a main test area (also referred to as target area), 2 control rooms and a buffer-area for storage¹. A layout drawing of the T8 beam-line and surrounding areas is shown in figure 2.1, and a photo of the test area is shown in 2.2. The control room is dedicated to monitoring the facility and has space for users to make dry-runs of their test set-up, whereas the technical-local is where the control and monitoring equipment for the users is installed during their tests. A separate platform outside the control room is available for testing large devices (full sized racks and large equipment) which connects directly with the control room for dry-testing. All the connections and cabling (including length) within the control match exactly those used between the test area and technical local, as to keep the dry-run set-up configuration exactly the same as with the real tests.

To perform a test, the users device is installed on a rack and moved to the test positions using an automated conveyor system (AVT). The test positions are shown in figure 2.4. The cabling for the test device is placed into a 'cable-order-chain' attached to a rail system and is moved in to place together with the conveyor. Figure 2.5 shows how the cables are arranged. Inside the test area there is a patch-panel with an array of different connections for the user to connect their equipment. These connections lead directly to a patch-panel inside the technical locale. A list of available cables and connectors can be found on the CHARM website: <http://charm.web.cern.ch/CHARM/Cables.php>

During operation the beam is directed on one of three targets; copper, aluminium and 'aluminium with holes'. By choosing different targets, the intensity of the radiation field can be varied, with the copper target generally giving the highest dose and particle fluences, and the 'aluminium with holes' target giving the least. For in beam measurements it is possible to run without target, so one can test in a pure proton field.

There are four layers of shielding installed in the middle of the area which can be moved in and out of place to tailor the radiation field. The outer two layers of 20cm thick concrete surround two layers of 20cm thick iron in a 'sandwich' arrangement. The 'concrete-iron-iron-concrete' layout is referred to as 'CIIC' for the facility configuration, where partial shielding and running without any shielding at referred to as 'CIOO' (concrete-iron-open-open) and 'OOOO' (all four open).

¹A more detailed description of the facility can be found in the safety file [reference].

Within the test area there are a number of different positions one can place test equipment in CHARM, which can either be directly in the proton beam, behind shielding or at various angles and distances from the target. By varying the target, shielding and position of the test device, a large number of radiation fields can be achieved. These are described in detail in chapter 3.

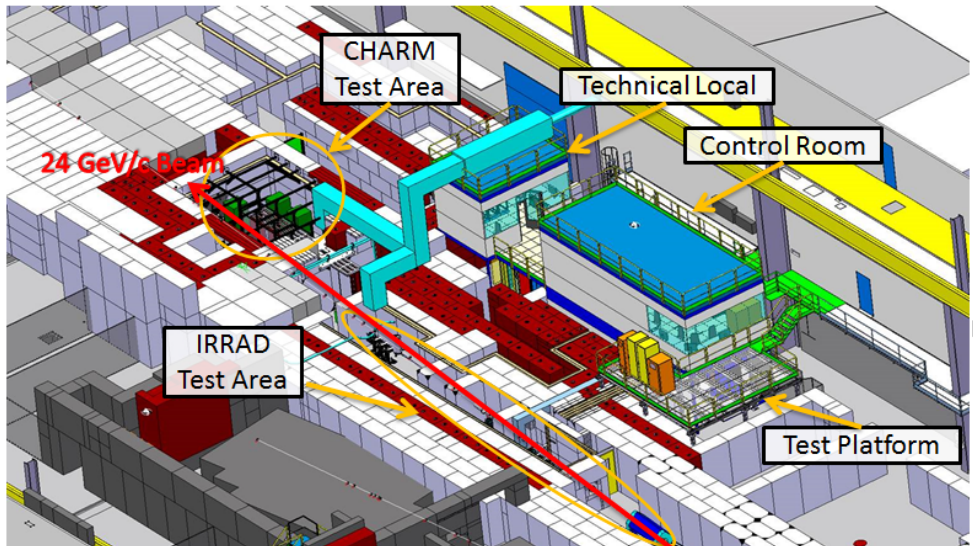


Figure 2.1: A screen-shot from the 3D Catia drawing of the IRRAD and CHARM facility, showing the different areas.



Figure 2.2: A photo of the test area. The moveable shielding is in the centre of the photo, with the target behind.

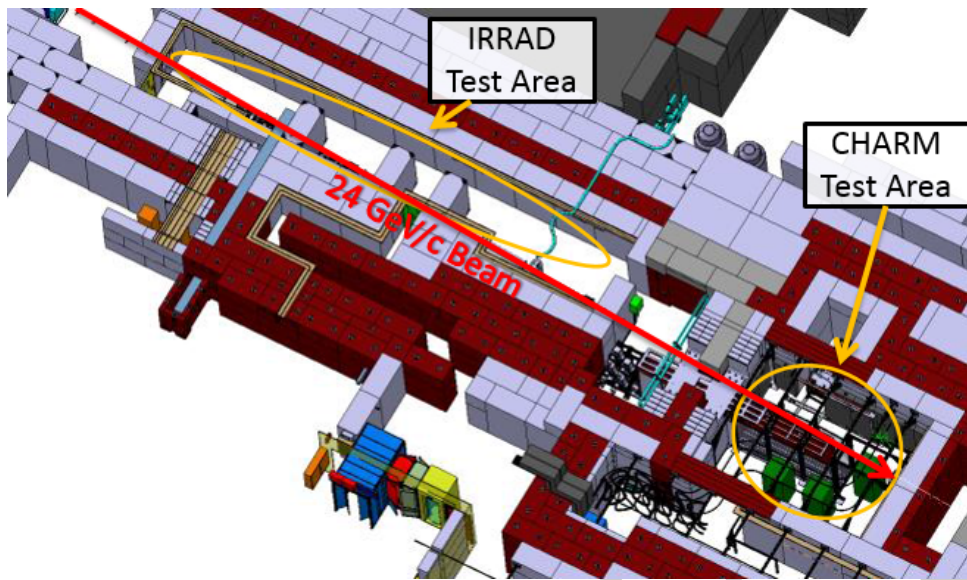


Figure 2.3: A screen-shot of the 3D Catia drawings for the T8 beam-line on the East Area hall showing the position of the IRRAD and CHARM facilities along the T8 beam-line.

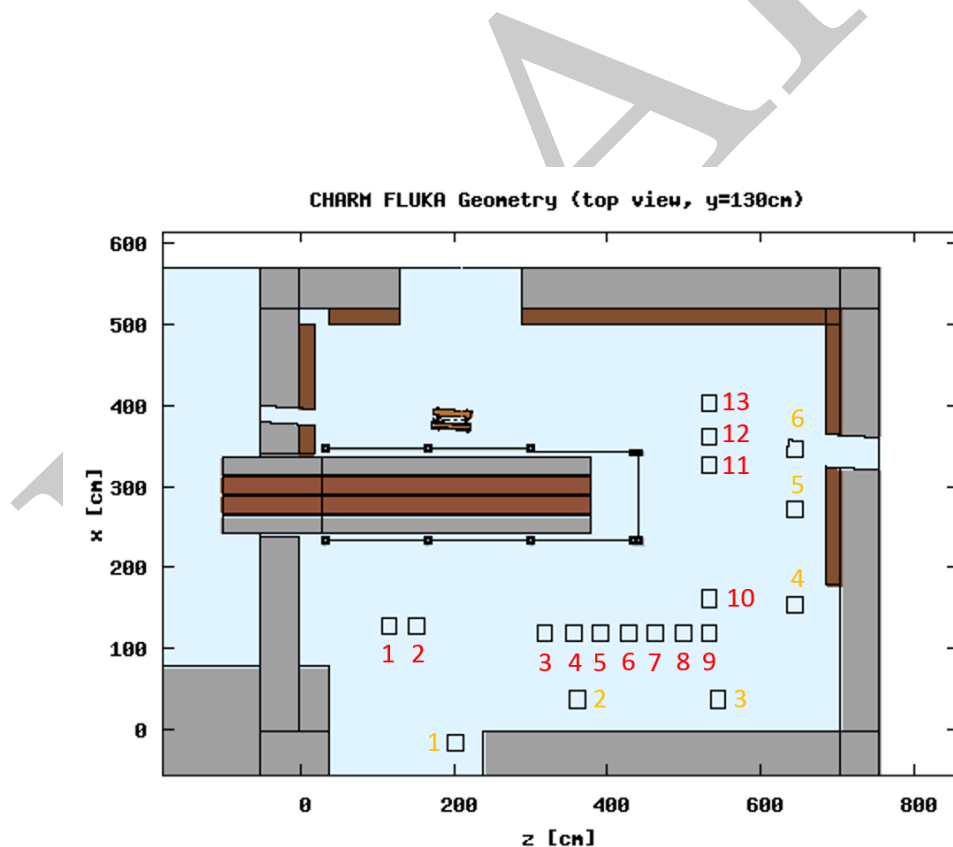


Figure 2.4: A screen-shot showing the test positions in the FLUKA geometry, cut at beam-height. The rack positions are numbered in red, and the Montrac test positions are numbered in yellow.

2.1 Facility Configuration

There are a number of possible ways to change the radiation field within the test area depending on the requirements of the users and the desired test environment. Below is a list of the options.

Targets

There are 3 targets for use in the test area; copper, aluminium and aluminium with holes. The first 2 are solid metal, however the third is made from machined disks of aluminium with cuts made through the centre, reducing the effective density along with middle by a factor 2, leading to less beam interaction. These are referred to as 'cp', 'al' and 'alh' respectively.

Shielding

Between the test positions and target inside the test area, there are 4 movable shielding plates, made of either concrete ('C') or iron ('I'). The configuration of the shielding is referred to in the calculations as the order starting closest to the target and going further away. An example is 'CIIC', which means all shielding is in place, alternatively there are 'CIOO' which means half shielding, and 'OOOO' which means no shielding being used.

Test Positions

These are the 'rack' test positions, for which a conveyor system will be used to move the racks filled with the test electronics. There are a total of 13 possible rack positions, which will be referred to as 'r1' to 'r13'. These are in the mixed-field. The positions shown in figure 2.4 and the coordinates relative to the FLUKA geometry are described in the appendix in table A.1.

Beam Conditions

The beam extracted from the PS can be altered in a number of ways to suit the needs of the users. Firstly considering the effective beam intensity reaching the facility, the spill size and frequency can be altered. This can be varied from around 1E11 up to 5E11 per spill with up to 6 spills per super-cycle, giving around a factor 10 range in intensity for the users. More details on the beam conditions are given in the following section.

In addition to the above, there are other special test positions available:

Montrac Positions

These are positions along the Montrac rail system where the shuttle can stop and one can leave the equipment to be irradiated. There are fewer positions than the usual test locations, but adds additional positions for smaller equipment that can be run in parallel with the large racks. A photo of the Montrac test location is shown in figure 2.6.

In-beam Position

In addition to the Montrac positions, it is possible to stop the shuttle directly in beam and leave equipment for testing.

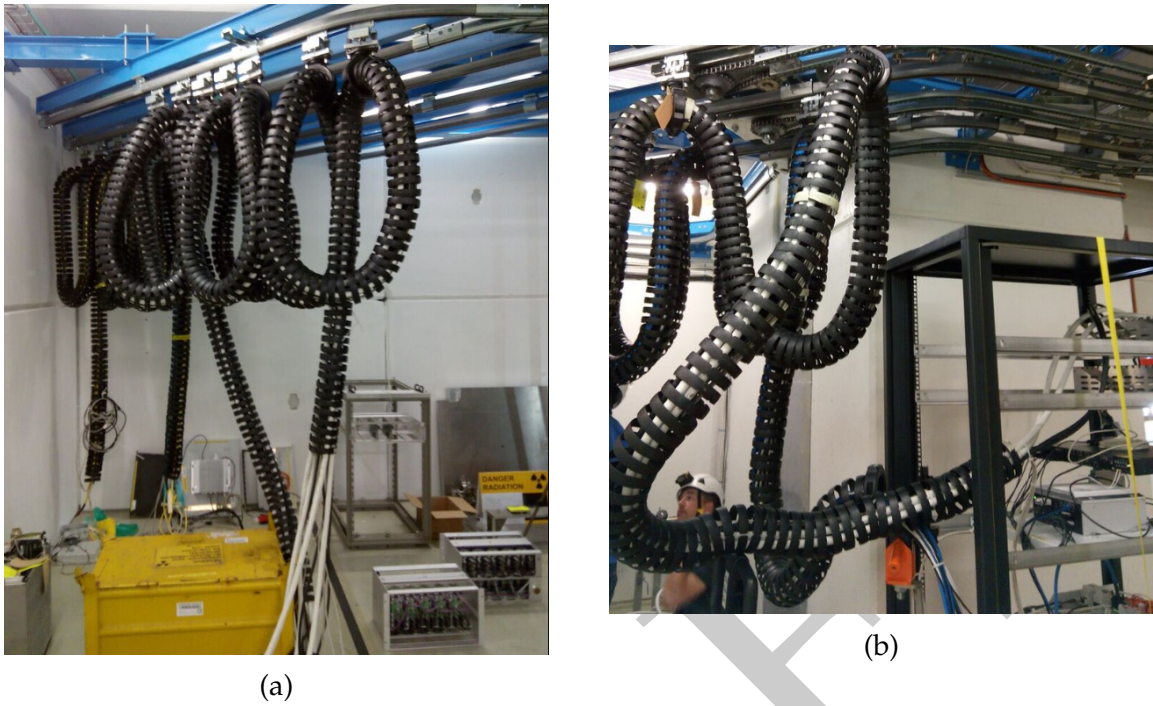


Figure 2.5: A photo of the cable-order-chain used to keep all the user cables together, and runs on a rail system making it easy to manipulate a potentially heavy mass of cables. Photo (a) shows the cable within the storage area, and photo (b) shows a test rack being connected to the cables.

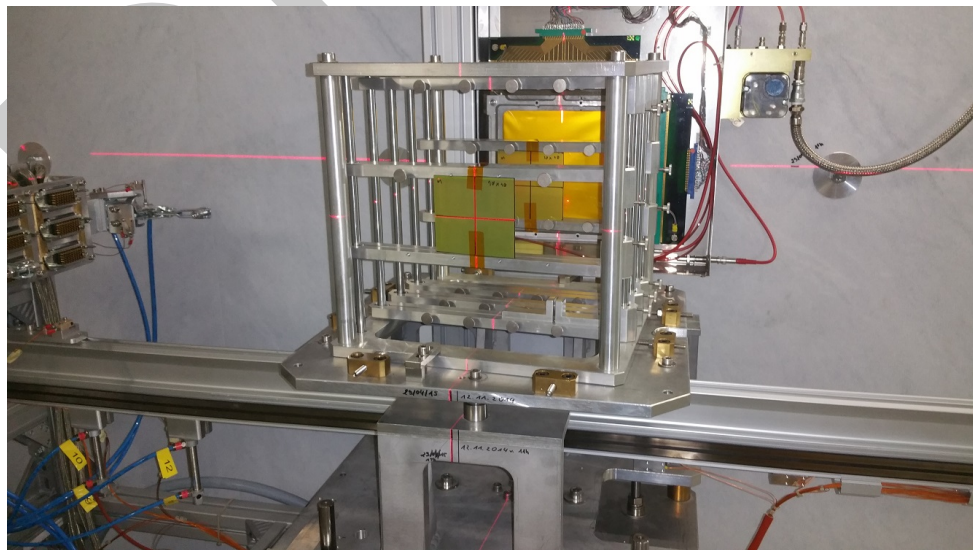


Figure 2.6: A photo of the Montrac test location with the test rack in place, ready for in-beam tests.

2.2 Beam Instrumentation

For monitoring the beam reaching the IRRAD and CHARM test facilities, there are a number of instruments that can be used to measure the beam intensity, position and size. All the available monitors are shown in figure 2.7. The instrumentation falls into 2 categories; **intensity monitoring**, and **position and beam size monitoring**.

2.2.1 Beam Intensity Monitoring

The beam intensity can be measured using either of the secondary emission counters (SEC1 and SEC2) or the ionisation chamber (IC). To determine the number of protons reaching the target (POT) at CHARM, the SEC1 detector is to be used as the reference. This detector is calibrated using the 'fast beam current transformer' (BCT) placed up-stream, just after the point of extraction from the PS. A cross-check is also made using activation foils.

During the SEC1 calibration test it was found.. [Eino's report, need conclusion].
SEC1 calibration = $2.\text{??}E7$ protons/count [error is..]

The SEC2 can also be used to measure the POT, however as this detector is positioned after the IRRAD facility, the signal can be influenced by sampled placed in beam at IRRAD. This has been observed during operation and can give misleading beam intensity measurements (reference), therefore it is recommended to use the SEC1 for POT calculations. The data from the SEC1, SEC2 and IC are all continuously logged in TIMBER. The variable names are listed in table 2.1.

2.2.2 Beam Position and Size Monitoring

The position of the beam can be measured as it passes through IRRAD using the 'beam position monitors' (BPM) (<https://ps-irrad.web.cern.ch/irrad/bpm.php>) and with the 'beam TV' (BTM) or 'multi-wire proportional chamber' (MWPC) as it passes CHARM. The BTM is only used to verify the beam position is correct after changes on the T8 beam-line. During operation the MWPC is used to monitor the beam shape and position. The detector is placed at the back of CHARM, just behind the Montrac test position. The data is logged in TIMBER under the variable names described in table 2.1.

2.3 Beam Specification

The CHARM facility receives a 24 GeV/c proton beam extracted from the CERN proton-synchrotron (PS), which is directed along the T8 beam-line in the PS East-Area Hall towards CHARM. The beam structure is in 'spills' (or bunches) separated by 1.2 seconds, organised in a 'super-cycle' usually of around 30 spills. This gives the beam a 'burst' like nature, as opposed to a constant beam without interruption. Each user of the beam

| Detector | TIMBER Variable Name |
|----------|------------------------|
| SEC1 | MSC01.ZT8.107:COUNTS |
| SEC2 | MSC02.ZT8.125:COUNTS |
| IC | ION01.ZT8.124:COUNTS |
| MWPC (x) | MWPC.ZT8.135:PROFILE_H |
| MWPC (y) | MWPC.ZT8.135:PROFILE_V |

Table 2.1: A table of the variable names as used in the logging database for the various beam instruments. The 'ZT8' refers to the T8 beam-line, and the number proceeding it refers to the distance of the detector to the beam extraction from the PS.

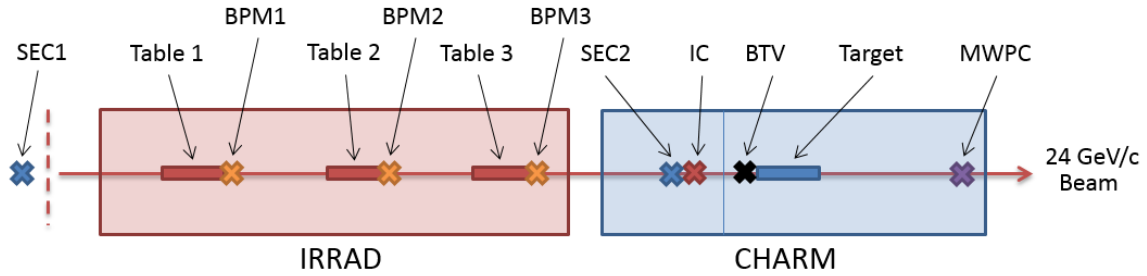


Figure 2.7: A diagram of the beam instrumentation for the T8 beam-line.

is allocated a specific spill (or several spills) and these are extracted individually to the respective beam-lines. An example of how the spills are typically arranged can be seen in figure 2.8.

The beam conditions for the T8 beam-line can vary based on the different parameters used from extraction down to the magnets preceding the IRRAD facility. For the cases when the target is being used, the beam will be focused on the target, with a FWHM of around 3cm. For direct irradiation in the beam, it is possible to enlarge the beam up to a FWHM of 10cm. More information about the beam parameters and conditions can be found in the T8 beam specification document [LAU 2014]. A summary of the usual beam conditions is shown in the next section.

2.4 Operating Conditions

During the initial test period, an analysis was made of the average beam intensity. It was possible to determine the average spill size and frequency, which can be used to make an estimate for the number of POT impinging the target over a set period. It was found that the average intensity seen on the SEC1 was 3.1E11 protons per spill. It was also noted that there was typically 3 spills per minute, which gives an average of around 1.8E10 protons per second, or 1.5E15 protons per day of running. This assumes no break in operation and no changes in the beam conditions. Therefore, to use

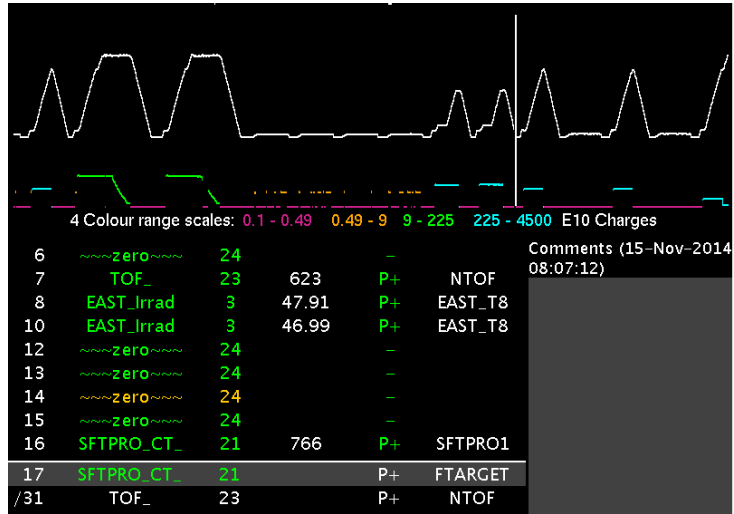


Figure 2.8: A screen-shot of the PS VISTAR page, giving live information about the beam extracted from the CERN PS. In this example, CHARM is receiving 2 spills (numbers 8 and 10) from a super-cycle of length 31 spills. The intensity measured at extraction in this case is around 4.7E11 protons per spill.

a reasonable scaling value for the remaining document, **1.5E15 protons per day** will be assumed when normalising datasets, and will be referred to hereafter as the nominal operation conditions.

During the same period it was noted that the spill frequency can be varied from 1 to 6 spills per minute, and the spill intensity can vary from 1.5E11 to around a maximum of 4.0E11 protons per spill. This gives the lower and upper running limits of around 2.1E14 to 2.3E15 protons per day respectively.

The beam size for irradiation with the target uses the normal beam conditions from the PS, which gives a beam-size of around 1 to 2cm FWHM. For in beam tests, it is possible to request the 'blown-up' beam setting from the PS operators. The reference for this was set during tests on 01/06/2015, and a beam of 8cm FWHM in the horizontal plane, and 12cm FWHM in the vertical was achieved. A plot of this on the MWPC is shown in figure 2.9. The values for the beam reference can be found in table 2.2.

The beam profile on the BPM1 was analysed for the test periods over November and December 2014 and an average made over all channels in the x and y planes. It was seen to have a Gaussian distribution, with a FWHM of 14.6mm and 10.7mm in x and y respectively. The profile differed slightly for BPM2 where the beam was larger in the y plane, with a FWHM of 11.5mm and 14.1mm in x and y respectively.

| Beam Setting | Units | x Plane | y Plane | Tolerance |
|---------------|-------|---------|---------|-----------|
| Target | mm | 22 | 22 | ± 3 |
| In-beam Tests | mm | 80 | 120 | ± 10 |

Table 2.2: Table of the reference beam settings for CHARM, as measured with the MWPC.

| Data | Units | Value | Tolerance |
|-----------------|-----------|----------|------------|
| PS Vista spills | spills/SC | 3 | ± 2 |
| SEC1 | p/spill | 3.60E+11 | $\pm 5E10$ |
| BPM1 (centre) | mm | 0 | ± 5 |
| BPM1 (sigma) | mm | 8 | ± 5 |
| MWPC (centre) | mm | 0 | ± 5 |
| MWPC (FWHM) | mm | 30* | ± 20 |

Table 2.3: A table of the typical parameters for the various monitors and detectors used at CHARM. These are for when the target is not in use.

* note this will increase to around 80mm when the target is in place.

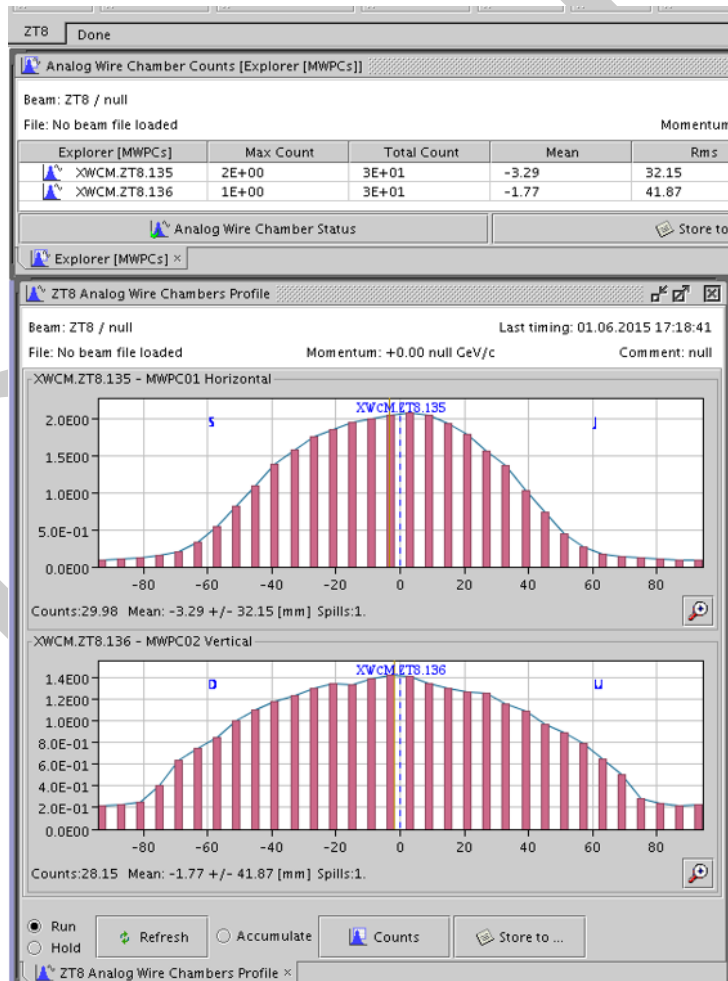


Figure 2.9: A screen-shot of the CESAR tool, showing the MWPC profile during the 'blown-up' beam reference conditions.

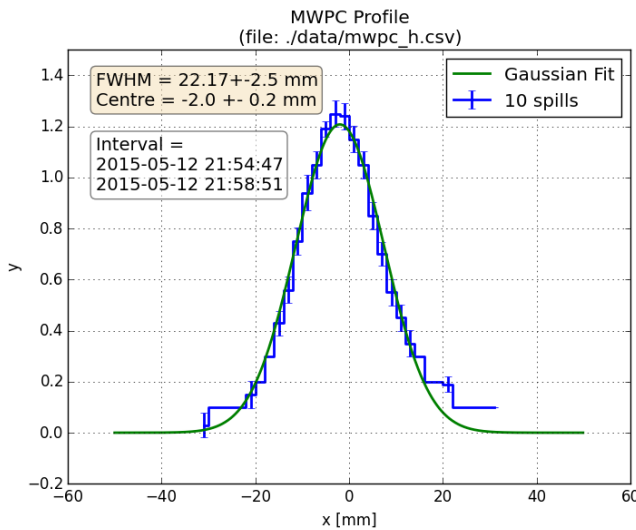


Figure 2.10: A plot of the horizontal beam profile captured with the MWPC during the commissioning period. This is the typical beam used with the target.

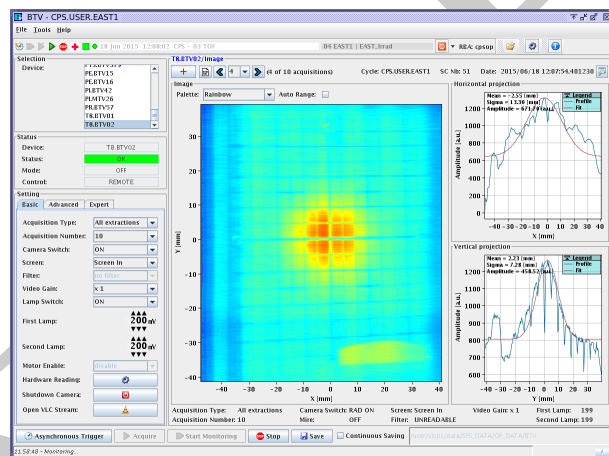


Figure 2.11: An example of the BTV acquisition from the PS operators showing the spill alignment. In this case, the beam was aligned perfectly.

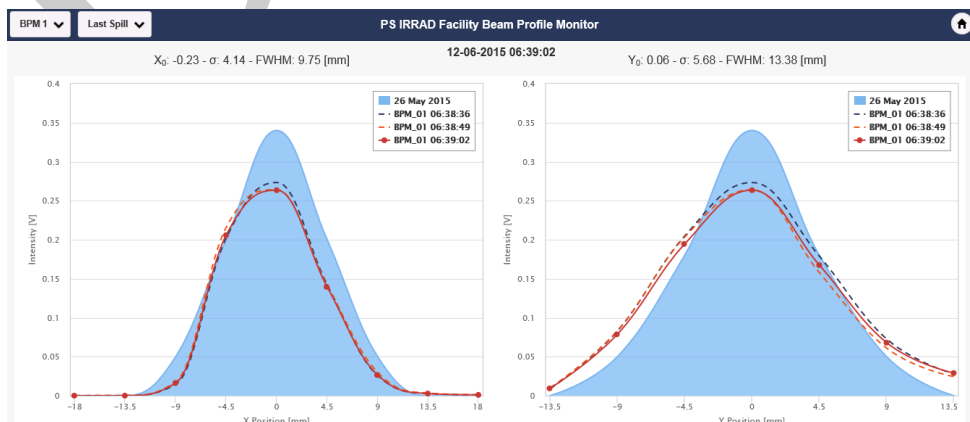


Figure 2.12: Example plots of the BPM1 from a typical testing period. The BPM1 is the reference when aligning the beam before using the target.

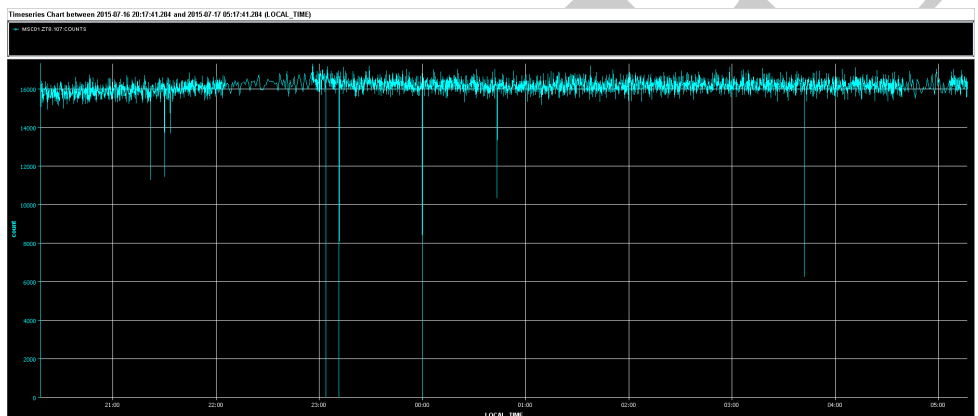


Figure 2.13: An example of the SEC1 signal acquired from TIMBER showing the beam intensity over a certain period.

Chapter 3

Radiation Field

This chapter describes the radiation field inside the CHARM test area. With the many different facility configurations, there is a large variation in the particle and energies seen in the spectra at the various test locations. In order to understand what the field is like in the different test positions, the FLUKA Monte Carlo code has been used to simulate the radiation field. This starts with making an accurate model of the inside of the test area, correctly describing the beam and making reasonable assumptions about the running of the facility.

In order to make a thorough and complete analysis of the radiation field, it is important to decide what information is needed, and how it can be compared with real-life mixed radiation fields such as space or accelerator facilities. This step requires the formation of metrics and standards, in order to make accurate comparisons and consider the strength of the match. From there, tables of data can be produced for each position and each configuration, stating the matches for various comparisons.

A list of useful units is included in the appendix, table B.2.

3.1 Quantifying the Radiation Field

There are many quantities which are useful to know during radiation tests, and these vary depending on the kind of test a user would like to make. It ranges from the simplest total ionising dose tests, where only the dose at the location as a function of time is needed, to very specific quantities such as 1MeV equivalent neutron fluence which is useful in studies of radiation damage in electronics.

The radiation environment inside the CHARM area is described to as a 'mixed' field. This means that the radiation within the test area comes in many types, such as protons, neutrons, pions, etc. These originate from the beam interacting with the target. This is contrary to a gamma facility for example, where the field is only 1 type of radiation. In fact many radiation environments can be described as a mixed-field, such as in the upper atmosphere where one finds not only protons but also neutrons and muons, thus the types of radiation are 'mixed'.

At CHARM one can find an entire range of particles from the beam interaction with the target. At the test location one typically sees a number of hadrons (including protons, neutrons, pions and kaons), leptons (electrons and positrons) and photons (x-ray and gamma). These range in energy from near primary beam protons and neutrons at 24 GeV, to thermal neutrons from the test area wall scattering at <1 eV.

3.2 Metrics

In order to compare the mixed-radiation field at CHARM with other fields, a metric needs to be decided in order to be able to describe and then compare radiation fields. This should give a clear and simple way to cross-compare, and should also show the strength of the fit. This could be either a single value, or a number of different tests that overall show the quality of the fit for that environment.

The first metric that could be used are the 'hardness factors', which quantify range of energies of high energy hadrons in a radiation environment. To calculate these factors, one takes the simulated high energy hadron spectrum and makes a reverse integral, normalised to 1 at 20MeV. From this, the values at 50% and 10% are taken, which correspond to the proportion of the HEH fluence above this energy.

A second way to make a comparison between datasets and real measurements could be to use the fission cross-section in Tungsten for devices where the material is used. The importance of Tungsten is from the fragments caused during fission reactions. These fragments have a large LET and thus deposit large amounts of charge, which maybe be close to the active volume of the electronics.

The method involves taking the simulated Tungsten fission cross-section and folding this with the simulated normalised HEH fluence. The integral of the folded spectrum will give the probability of a fission event in Tungsten for this HEH spectrum. For a comparison with a real value, one can divide this by the 230 MeV proton induced fission cross-section in Tungsten. Then, if one tests a device in a 230 MeV proton beam, the ratio will give an indication of how the number of events could scale in the simulated HEH spectrum. An example of this method is shown in figure 3.1, which gives a ratio of 1.322 between the cross-section at 230 MeV and the expected cross-section in the mixed-field at this location and configuration.

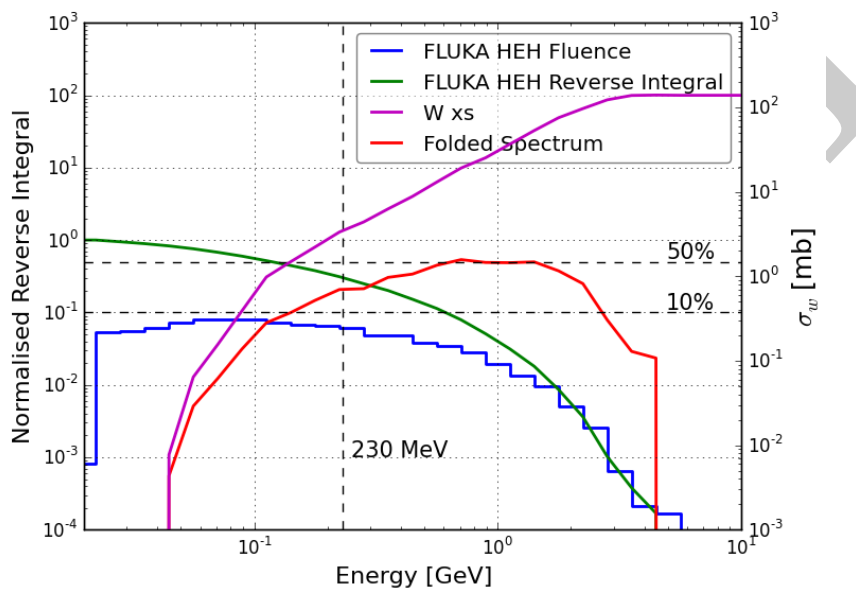


Figure 3.1: A plot of the HEH fluence for a specific test position, folded with the Tungsten fission-fragment cross-section, giving a 'response' for a detector in which the SEU sensitivity is dominated by the Tungsten inside the device. A reference of 230 MeV is used to compare with results with those obtained during tests at PSI in Switzerland. Also plotted is the HEH reverse integral spectra, with the corresponding H10 and H50 factors.

3.3 Standards and Environments

There are a number of different environments (natural or otherwise) which have been studied to calculate the radiation field. The different radiation types, energies and fluences are calculated for each environment and tabulated, but to be able to compare them, some standards have to be created. As shown in the previous section, one way to compare different mixed-field radiation environments is to use the 'hardness-factor' which is related to the fluence of high-energy hadrons, and gives information about the energy and flux of hadrons. A collection of these values, including spectral information is shown in table 3.1. The data for the various LHC areas is given for nominal conditions (50fb^{-1}).

For TID testing, there are a range or standard dose rates... (need table) ELDR..

Description and reference to some different environments (spectra plots?)

| Environment | HEH /cm ² / y | Composition (%) | | | | R | Hardness Energy | | |
|-----------------------------|-----------------------------|-----------------|----|------------------|------------------|------|-----------------|------|------|
| | | n | p | pi ⁺⁻ | n _{int} | | H50 | H10 | H1 |
| CERN - LHC UJ | 2.5E+09 | 99 | 1 | 0 | 32 | 2 | 0.08 | 0.18 | 0.36 |
| CERN - LHC RR | 1.0E+09 | 71 | 13 | 16 | 25 | 10 | 0.18 | 0.69 | 2.8 |
| CERN - LHC Tunnel | 6.0E+11 | 45 | 18 | 37 | 19 | 2.8 | 0.37 | 1.8 | 5.7 |
| CERN - ATLAS Outer Tracker | 3.5E+09 | 67 | 5 | 28 | 25 | 1.1 | ? | 0.46 | 0.71 |
| CERN - ATLAS Inner Tracker | 1.0E+12 | 4 | 7 | 89 | 1 | 2 | 1.5 | 3.8 | 12 |
| CERN - LINAC 4 | 1.0E+10 | 99 | 1 | 0 | 86 | 1.5 | ? | 0.07 | 0.1 |
| CERN - PS | 1.0E+11 | 61 | 17 | 22 | 19 | 4.9 | ? | 0.9 | 2.4 |
| CERN - SPS | 1.0E+12 | 70 | 12 | 18 | 29 | 48.9 | ? | 0.94 | 5.1 |
| QARM - 350m (Geneva, CH) | 1.6E+05 | 93 | 7 | 0 | 21 | 0.12 | 0.08 | 0.34 | 1.3 |
| QARM - 10km (Geneva, CH) | 1.7E+07 | 82 | 18 | 0 | 18 | 0.08 | ? | 0.92 | 5 |
| QARM - 20km (Geneva, CH) | 3.8E+07 | 68 | 32 | 0 | 14 | 0.06 | 0.5 | 2.9 | 13 |
| CREME 96 - ISS (450km) | 7.3E+08 | - | - | - | - | - | ? | 0.25 | 0.53 |
| CREME 96 - Proba II (800km) | 2.7E+09 | - | - | - | - | - | 0.1 | 0.28 | 1.5 |

Table 3.1: Table of hardness energies for various radiation environments. [NSREC Short-course]

3.4 FLUKA Calculations

The FLUKA Monte Carlo code (reference) was used to perform the radiation field calculations for the CHARM test area. For this, a geometry was built specifically for CHARM test area. This geometry includes all the main features of the test area; i.e. the target table with the 3 different targets, the movable shielding, the different materials in the surrounding shielding walls, the exact test positions etc. An effort was made to make the geometry as accurate as possible with respect to the technical drawings and double-checked with measurements made in the facility, in order to reduce the errors with respect to positioning. Care needed to be taken as the variations in the radiation field with respect to position (gradients) can be high for areas close to the beam and down-stream of the target.

3.4.1 FLUKA Geometry

An accurate model was made specifically using FLUKA for the CHARM area. Details and dimensions were taken from a combination of CATIA 3D drawings, and then finally measurements once the facility had been constructed. It was decided to focus on the details around the test area, therefore the geometry as seen in FLUKA includes only the first layer of shielding. This will optimise the time used during the calculations by not tracking the particles in area that are not of interest.

The co-ordinate system for the FLUKA geometry was defined with the z axis parallel with the beam, y axis for the height, and the x axis adjacent to the beam. This will then be used in the rest of the document when describing the radiation field. These along with the test positions can be seen in figure 2.4.

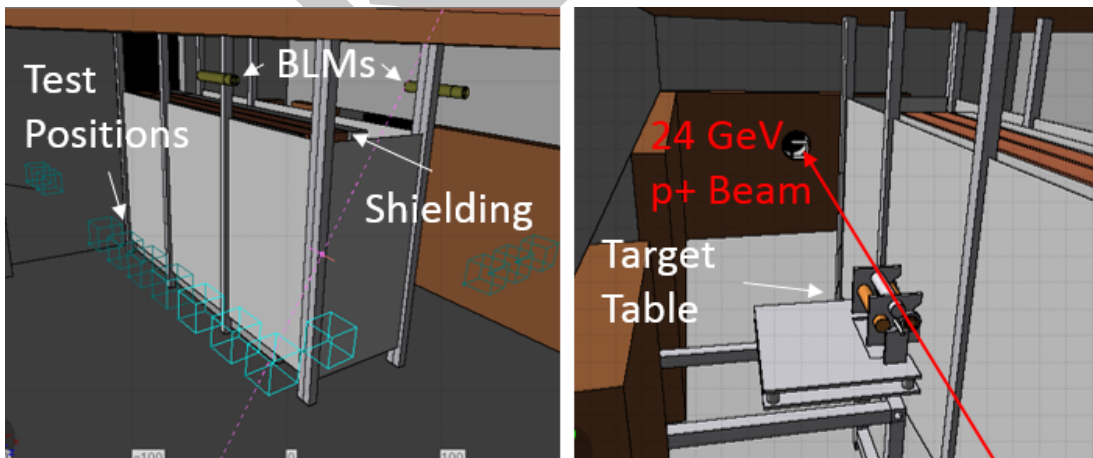
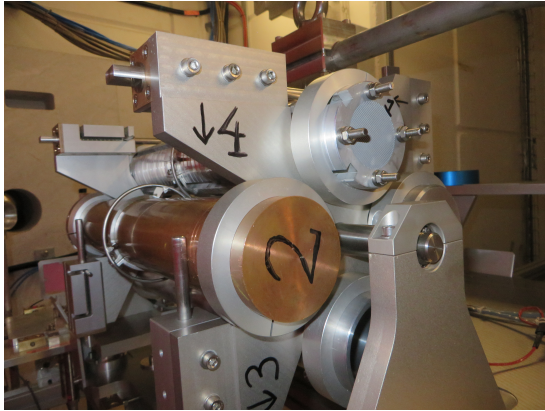
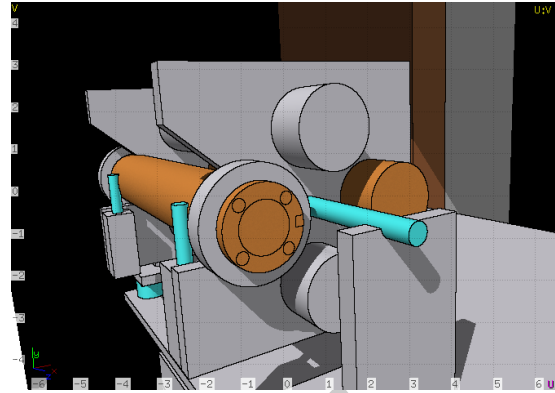


Figure 3.2: A screen-shot of a cut of the FLUKA geometry, showing the shielding and test position scorings (in blue). The BLMs are also visible at the top of the shielding.



(a) A photo of the target table.



(b) A screen-shot from the FLUKA geometry

Figure 3.3: A comparison of the real target station and the simplified target station implemented in the FLUKA geometry.

3.4.2 Scoring

There are a number of estimators built into FLUKA for calculating various quantities, such as charge particle fluence, dose in air etc. Deciding which estimators to use and how to normalise the data depends on the purpose of the simulation. For the CHARM facility, the focus is on testing of electronics, for which there are a number of appropriate estimators for this purpose. One example is scoring 'high-energy hadrons' i.e. the total flux of hadrons above 20 MeV (deemed the cut-off energy for SEE's in electronics). The selection used for the CHARM FLUKA studies is listed below.

| Estimator | Physical Meaning |
|-----------|---|
| DOSE | The energy deposited per unit mass |
| HADGT20M | Fluence of Hadrons with energy above 20 MeV |
| SI1MEVNE | Fluence of 1 MeV (Si) equivalent neutrons |
| NEUTRON | Fluence of neutrons |
| HEHAD-EQ | Fluence of Hadrons with energy above 20 MeV including intermediate neutrons |
| THNEU-EQ | Fluence of thermal-equivalent neutrons |

Table 3.2: A table of the estimators used for the CHARM FLUKA calculations. A detailed list can be found in the appendix in table X. More details available in the FLUKA manual.

Chapter 4

FLUKA Results

Using FLUKA to model the CHARM facility, it is possible to calculate the radiation field at the various test positions with all possible facility configurations: something that would be very difficult and could potentially take months for actual measurements. This chapter attempts to summarise the results for the test positions and Montrac location for a variety of configurations. It goes on to give more detail specifically for the 'cp_OOOO' configuration as this is a common choice by users of the facility. The tables and information presented for this configuration are also included for all other configurations in the appendix.

From the FLUKA calculations results there are a number different types of information at the test positions. The first of interest is the integral values: dose or particle fluence at that specific location for example. These are useful for simple tests relating to subjects such as tolerance to dose or certain particle types. The second is the fluence of different particles with respect to energy (spectral information) for each of the test positions. This can be used to explore effects correlated with energy, for example the effect of high energy particles on the response of the detector by placing in positions of low and high average particle energy (such as the hardness factor, mentioned in the previous chapter).

4.1 Overview

High-Energy Hadrons

The fluence of high-energy hadrons for the test positions perpendicular to the target can be reduced by a factor 5 using the half-shielding, and by a factor 10 using the full-shielding, as shown in figure 4.2.

The values for the 1% (H1), 10% (H10) and 50% (H50) hardness factors can be found in tables 4.1, 4.2 and 4.3 respectively. It is observed that the hardness factor generally increases as the positions move closer to the down-stream positions. This can be explained by the angle with respect to the target, as the secondary particles with a smaller scattering angle will have a higher energy, and those with a large angle will have a lower energy. The hardness factor does not vary highly between targets for the same shielding configuration, and remains almost the same for the positions perpendicular

to the beam. The test positions in the beam axis tend to have much higher hardness factors, especially those which are positioned beyond the shielding.

The H₅₀ factor is generally very similar between the aluminium targets, and tends to be slightly higher than that for the copper for the same positions and shielding configurations. This may be explained for the test positions down-stream of the target by a lower number of protons interacting with the target due to the lower density, and thus more protons with higher energy reaching the test positions. Overall it is observed that the shielding reduces the hardness factors by a factor 2 for the test positions adjacent to the beam.

In terms of HEH fluence, it is possible to emulate many different radiation environments within the CHARM test area. The plot in figure 4.1 shows the reverse integral spectra for several radiation environments compared to those at different test positions, marked in grey. A table of the hardness factors for different environments are given in figure 3.1 [NSREC Short Course doc].

Dose

In the CHARM test area is it possible to expose test equipment to a large range of doses, depending on the target, shielding, and test position. The results in table 4.4 show the different dose rates possible per day (normal beam conditions) for the different variations of the facility configuration.

The lowest doses are observed unsurprisingly with the full shielding and aluminium target (with holes). As this is the least dense target, interaction of the beam with the target is the lowest of the different target options, and therefore the number of secondary particles created with the same number of incoming primary protons is lower. The number of secondary particles can be considered proportional to the dose, however this also depends on the particle type and energy, which will be discussed later in the report. For this facility configuration, the lowest dose is observed at the test positions with the highest angle relative to the beam line, where the fluence of secondaries again would be the lowest.

The highest doses are seen at test position 12 (irrespective of shielding, as this position is in line of sight with the target) with the aluminium target with holes. As this target is the least dense, the number of interactions is the lowest of the targets (as stated before). Therefore a large number of primary protons which will directly pass the target with minimal interaction, and therefore with the highest energy and fluence. This would lead to a greater dose deposited on the test equipment.

Considering the different shielding configurations, table 4.4 generally shows a factor 10 reduction in the dose seen at the shielded test positions between the cases of full shielding and no shielding. The case for half shielding is not shown, however a reduction in dose of around 50% is observed between full and half shielding cases.

The plot in figure 4.3 shows the dose for a slice in the CHARM FLUKA geometry, running from the target towards the entrance wall and highlights the reduction in the

dose rate for the different shielding configuration with the copper target. Directly after the shielding a reduction of almost 100 is observed between the cases with and without shielding, which reduces down to a factor of 10 by the test positions around $x = 120$ cm.

LET and particle types? How does one calculate dose for there application? How does this compare with FLUKA?

| Rack | No Shielding | | | Half Shielding | | | Full Shielding | | |
|------|--------------|-------|-------|----------------|-------|-------|----------------|-------|-------|
| | cp | al | alh | cp | al | alh | cp | al | alh |
| 1 | 0.38 | 0.39 | 0.39 | 0.31 | 0.30 | 0.30 | 0.30 | 0.28 | 0.28 |
| 2 | 0.41 | 0.43 | 0.43 | 0.32 | 0.30 | 0.30 | 0.32 | 0.29 | 0.29 |
| 3 | 0.69 | 0.73 | 0.72 | 0.50 | 0.49 | 0.48 | 0.45 | 0.38 | 0.39 |
| 4 | 0.78 | 0.80 | 0.81 | 0.58 | 0.56 | 0.55 | 0.48 | 0.44 | 0.42 |
| 5 | 0.89 | 0.92 | 0.92 | 0.64 | 0.62 | 0.61 | 0.50 | 0.45 | 0.47 |
| 6 | 0.99 | 1.01 | 1.01 | 0.73 | 0.72 | 0.69 | 0.56 | 0.49 | 0.49 |
| 7 | 1.12 | 1.16 | 1.16 | 0.79 | 0.77 | 0.76 | 0.57 | 0.55 | 0.55 |
| 8 | 1.23 | 1.26 | 1.27 | 0.88 | 0.85 | 0.83 | 0.63 | 0.61 | 0.61 |
| 9 | 1.38 | 1.42 | 1.43 | 0.95 | 0.90 | 0.90 | 0.70 | 0.70 | 0.70 |
| 10 | 1.67 | 1.73 | 1.72 | 1.08 | 1.04 | 1.01 | 0.90 | 0.91 | 0.90 |
| 11 | 12.57 | 14.34 | 14.63 | 12.47 | 14.24 | 14.57 | 12.48 | 14.26 | 14.57 |
| 12 | 24.00 | 24.00 | 24.00 | 24.00 | 24.00 | 24.00 | 24.00 | 24.00 | 24.00 |
| 13 | 6.51 | 7.21 | 7.27 | 6.31 | 7.14 | 7.22 | 6.32 | 7.14 | 7.23 |

Table 4.1: A Table of the H1 hardness factors for the different target and shielding configurations.

| Rack | No Shielding | | | Half Shielding | | | Full Shielding | | |
|------|--------------|-------|-------|----------------|-------|-------|----------------|-------|-------|
| | cp | al | alh | cp | al | alh | cp | al | alh |
| 1 | 0.18 | 0.19 | 0.19 | 0.16 | 0.15 | 0.15 | 0.16 | 0.15 | 0.15 |
| 2 | 0.19 | 0.20 | 0.20 | 0.16 | 0.16 | 0.16 | 0.17 | 0.16 | 0.15 |
| 3 | 0.31 | 0.34 | 0.34 | 0.23 | 0.22 | 0.22 | 0.21 | 0.19 | 0.19 |
| 4 | 0.36 | 0.39 | 0.39 | 0.25 | 0.24 | 0.24 | 0.22 | 0.20 | 0.19 |
| 5 | 0.41 | 0.44 | 0.44 | 0.28 | 0.26 | 0.26 | 0.22 | 0.20 | 0.20 |
| 6 | 0.47 | 0.49 | 0.49 | 0.30 | 0.29 | 0.28 | 0.23 | 0.21 | 0.21 |
| 7 | 0.51 | 0.56 | 0.56 | 0.32 | 0.30 | 0.30 | 0.23 | 0.22 | 0.22 |
| 8 | 0.58 | 0.62 | 0.62 | 0.34 | 0.33 | 0.31 | 0.24 | 0.24 | 0.24 |
| 9 | 0.63 | 0.68 | 0.69 | 0.36 | 0.34 | 0.33 | 0.26 | 0.27 | 0.26 |
| 10 | 0.78 | 0.85 | 0.85 | 0.39 | 0.38 | 0.38 | 0.33 | 0.34 | 0.33 |
| 11 | 6.84 | 8.15 | 8.55 | 6.64 | 8.01 | 8.45 | 6.63 | 8.02 | 8.45 |
| 12 | 23.00 | 24.00 | 24.00 | 22.95 | 24.00 | 24.00 | 22.95 | 24.00 | 24.00 |
| 13 | 3.35 | 3.87 | 3.90 | 3.21 | 3.81 | 3.85 | 3.22 | 3.81 | 3.85 |

Table 4.2: A Table of the H10 hardness factors for the different target and shielding configurations.

| Rack | No Shielding | | | Half Shielding | | | Full Shielding | | |
|------|--------------|-------|-------|----------------|-------|-------|----------------|-------|-------|
| | cp | al | alh | cp | al | alh | cp | al | alh |
| 1 | 0.06 | 0.07 | 0.07 | 0.06 | 0.06 | 0.06 | 0.07 | 0.06 | 0.06 |
| 2 | 0.06 | 0.07 | 0.07 | 0.06 | 0.06 | 0.06 | 0.07 | 0.06 | 0.06 |
| 3 | 0.09 | 0.10 | 0.10 | 0.08 | 0.08 | 0.07 | 0.08 | 0.07 | 0.07 |
| 4 | 0.10 | 0.11 | 0.11 | 0.08 | 0.08 | 0.08 | 0.08 | 0.07 | 0.07 |
| 5 | 0.11 | 0.12 | 0.12 | 0.09 | 0.08 | 0.08 | 0.07 | 0.07 | 0.07 |
| 6 | 0.12 | 0.13 | 0.13 | 0.09 | 0.09 | 0.08 | 0.07 | 0.07 | 0.07 |
| 7 | 0.13 | 0.14 | 0.14 | 0.09 | 0.09 | 0.09 | 0.07 | 0.07 | 0.07 |
| 8 | 0.14 | 0.16 | 0.15 | 0.09 | 0.09 | 0.09 | 0.07 | 0.07 | 0.07 |
| 9 | 0.15 | 0.17 | 0.17 | 0.09 | 0.09 | 0.09 | 0.07 | 0.08 | 0.08 |
| 10 | 0.19 | 0.21 | 0.21 | 0.09 | 0.09 | 0.09 | 0.08 | 0.08 | 0.08 |
| 11 | 1.79 | 2.69 | 2.87 | 1.57 | 2.56 | 2.76 | 1.57 | 2.55 | 2.76 |
| 12 | 7.01 | 20.42 | 21.59 | 6.72 | 20.40 | 21.59 | 6.72 | 20.40 | 21.59 |
| 13 | 0.73 | 1.20 | 1.25 | 0.60 | 1.11 | 1.18 | 0.60 | 1.11 | 1.18 |

Table 4.3: A Table of the H50 hardness factors for the different target and shielding configurations.

| Rack | No Shielding | | | Full Shielding | | |
|------|--------------|----------|----------|----------------|----------|----------|
| | cp | al | alh | cp | al | alh |
| 1 | 2.48e+16 | 9.41e+15 | 5.46e+15 | 1.52e+15 | 6.89e+14 | 4.64e+14 |
| 2 | 2.71e+16 | 1.06e+16 | 6.23e+15 | 1.70e+15 | 8.30e+14 | 5.23e+14 |
| 3 | 5.12e+16 | 2.22e+16 | 1.28e+16 | 2.92e+15 | 1.89e+15 | 1.29e+15 |
| 4 | 5.15e+16 | 2.34e+16 | 1.34e+16 | 3.18e+15 | 2.51e+15 | 1.53e+15 |
| 5 | 4.75e+16 | 2.39e+16 | 1.35e+16 | 3.91e+15 | 3.02e+15 | 1.86e+15 |
| 6 | 5.18e+16 | 2.66e+16 | 1.52e+16 | 4.29e+15 | 3.53e+15 | 2.15e+15 |
| 7 | 5.09e+16 | 2.74e+16 | 1.58e+16 | 4.56e+15 | 4.29e+15 | 2.70e+15 |
| 8 | 4.85e+16 | 2.82e+16 | 1.62e+16 | 5.38e+15 | 5.14e+15 | 3.28e+15 |
| 9 | 4.65e+16 | 2.90e+16 | 1.66e+16 | 6.15e+15 | 6.35e+15 | 3.86e+15 |
| 10 | 5.41e+16 | 3.89e+16 | 2.23e+16 | 8.91e+15 | 1.02e+16 | 6.26e+15 |
| 11 | 1.21e+17 | 3.79e+17 | 2.56e+17 | 1.19e+17 | 3.86e+17 | 2.60e+17 |
| 12 | 2.36e+17 | 1.08e+18 | 1.26e+18 | 2.39e+17 | 1.08e+18 | 1.26e+18 |
| 13 | 1.01e+17 | 2.30e+17 | 1.34e+17 | 1.06e+17 | 2.34e+17 | 1.36e+17 |

Table 4.4: A Table of dose per day for the different target and shielding configurations.

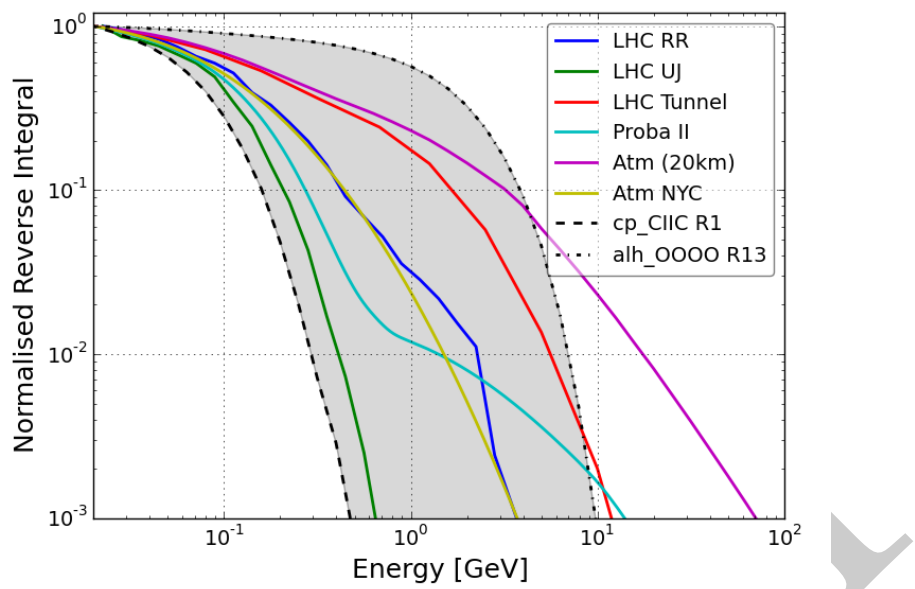


Figure 4.1: A plot of the reverse integral spectra for test positions at CHARM (in grey), compared with different radiation environments, normalised to 20 MeV.

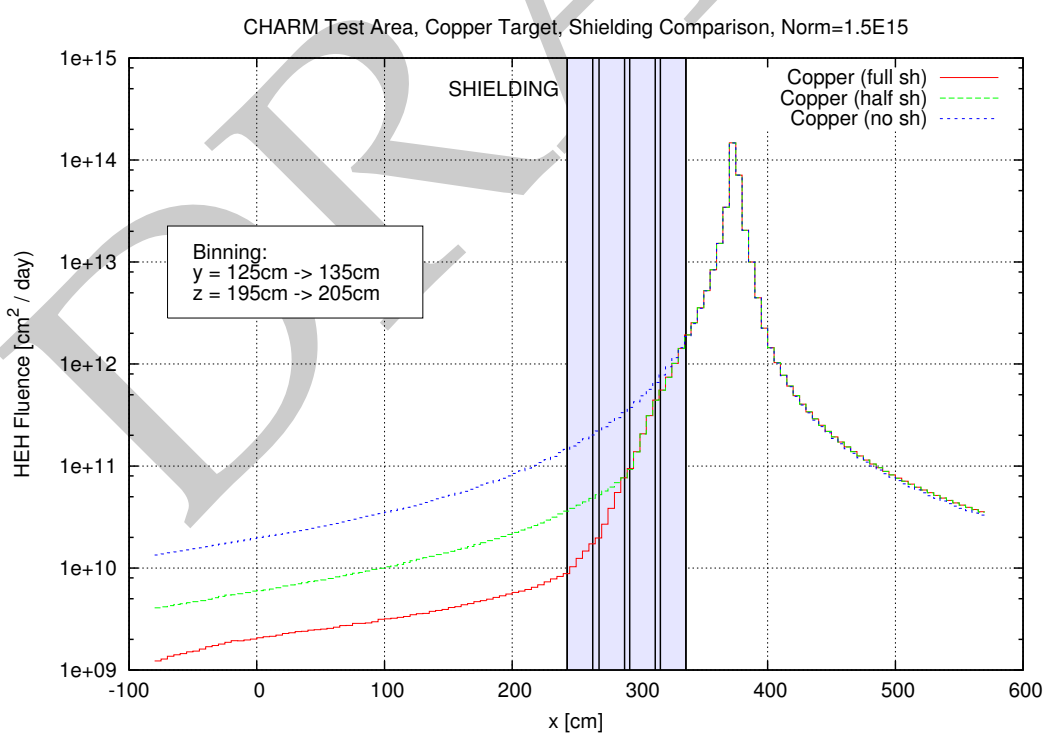


Figure 4.2: A plot of the HEH fluence for a slice in the test area geometry from the target, towards the entrance. It shows that with the shielding, there is a reduction in the HEH fluence of a factor 10.

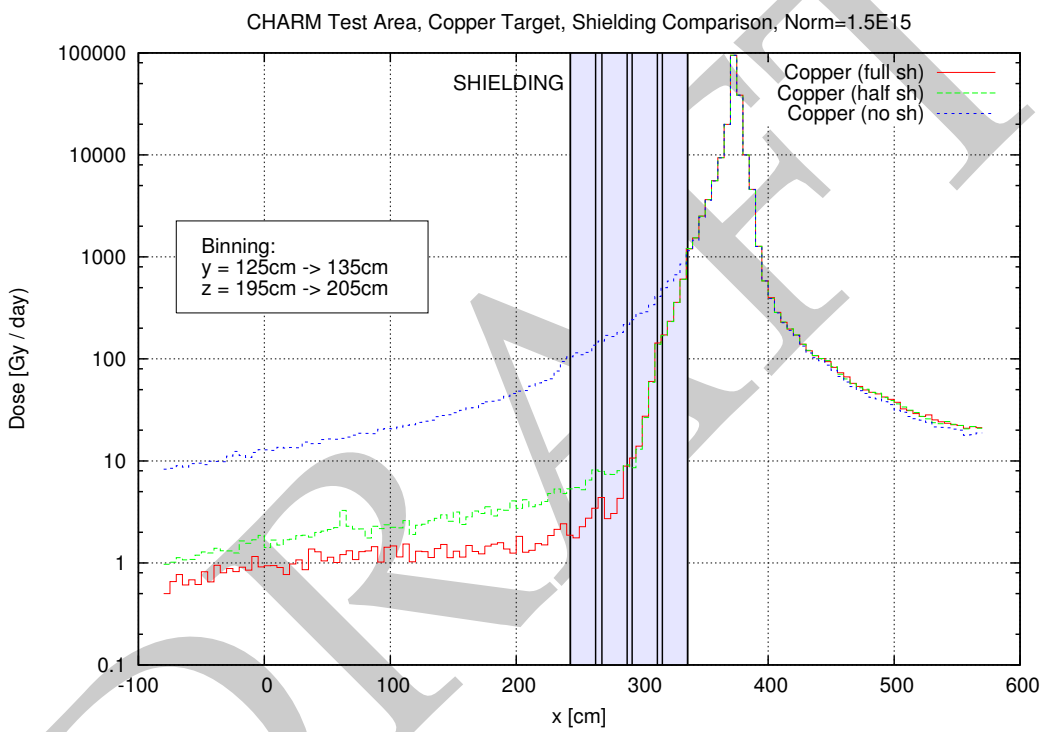


Figure 4.3: A plot of the dose for a slice in the test area geometry from the target, towards the entrance. The shielding reduces the dose by almost a factor 100 close to the shielding, and reduces down to a factor 10 by the test positions.

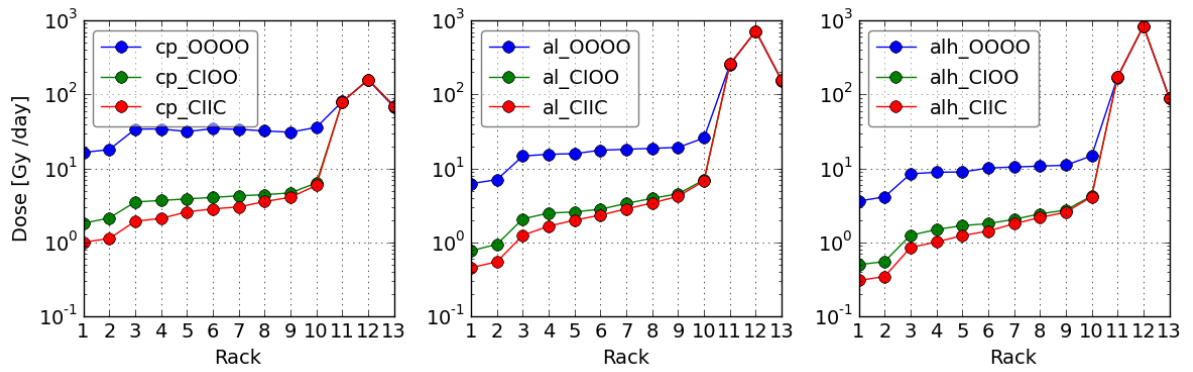


Figure 4.4: A plot of the dose per day at the different test positions with the different facility configurations.

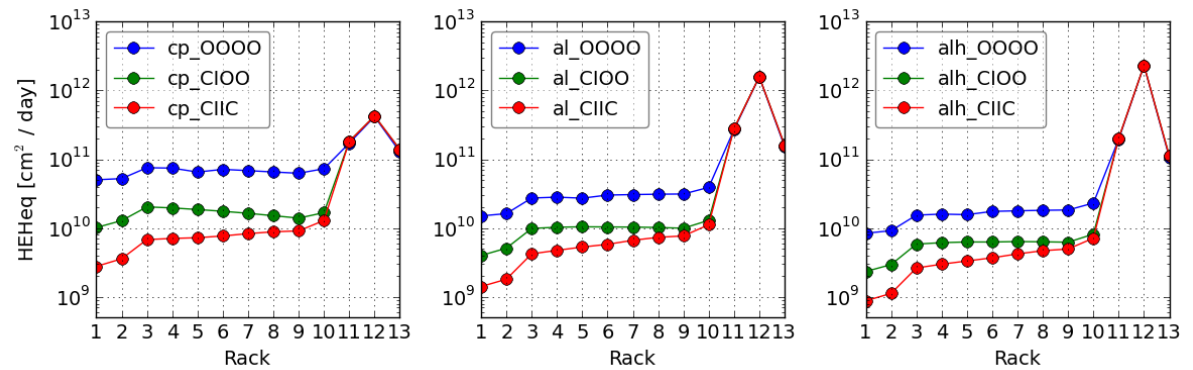


Figure 4.5: A plot of the high energy hadron fluence per day at the different test positions with the different facility configurations.

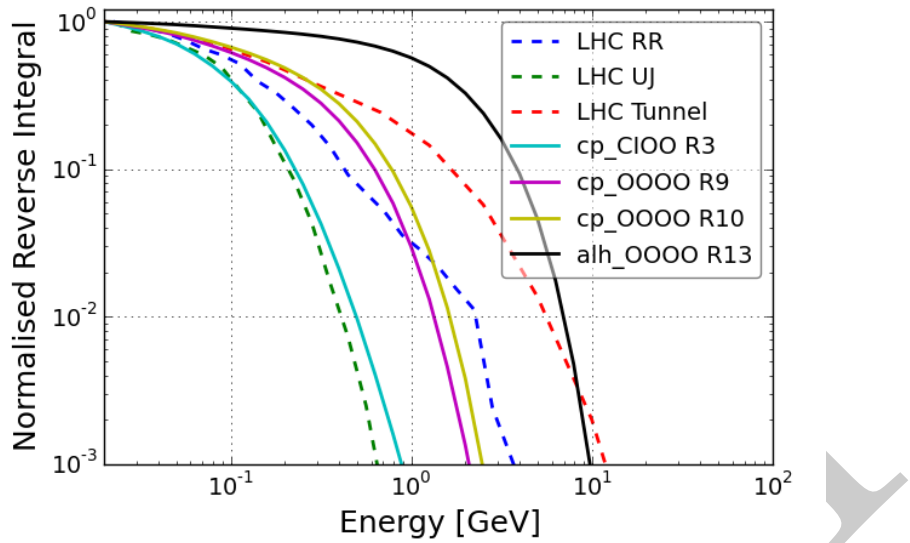


Figure 4.6: A plot of several reverse integral spectra from simulations of LHC environments, along with matching CHARM test configurations.

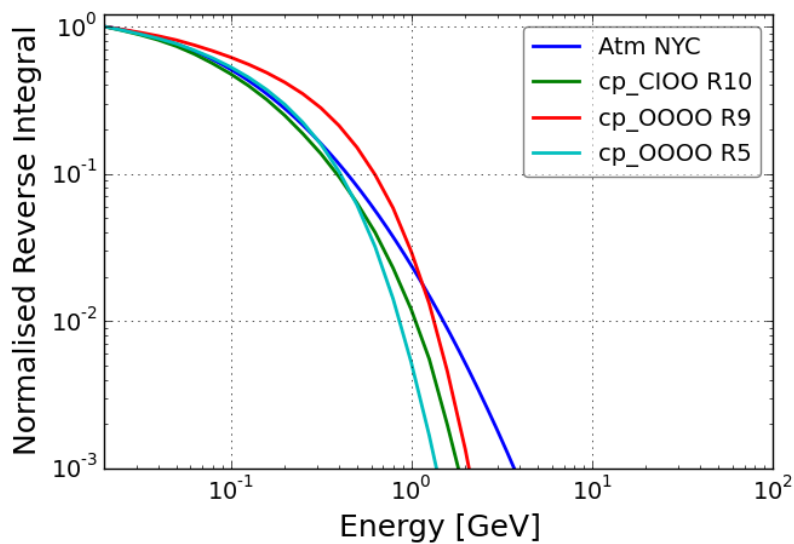


Figure 4.7: A plot of the reverse integral HEH spectrum at ground level (New York, Jedece89 Standard), with a number of CHARM test configurations with close matches.

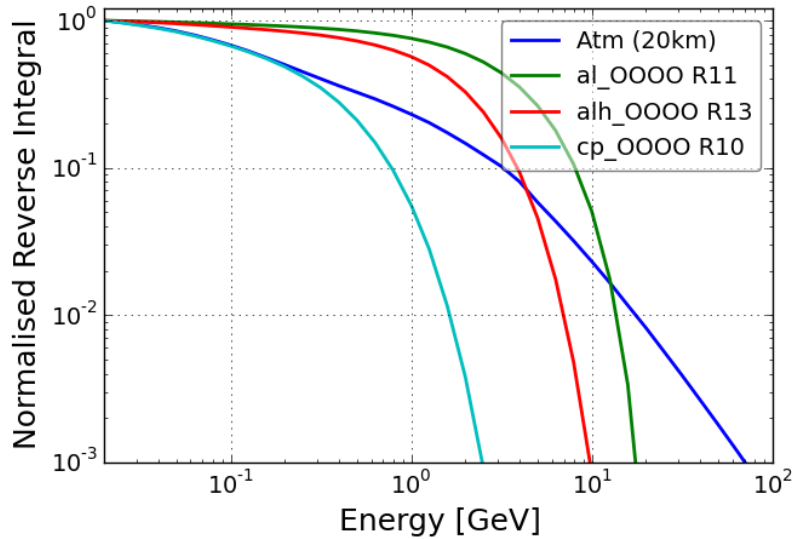


Figure 4.8: A plot of the reverse integral HEH spectrum at an altitude of 20km (Geneva, Switzerland), with a number of CHARM test configurations with close matches. The atmospheric HEH spectra extends to energies beyond those achievable at CHARM, however the intermittent hardness energies can be matched.

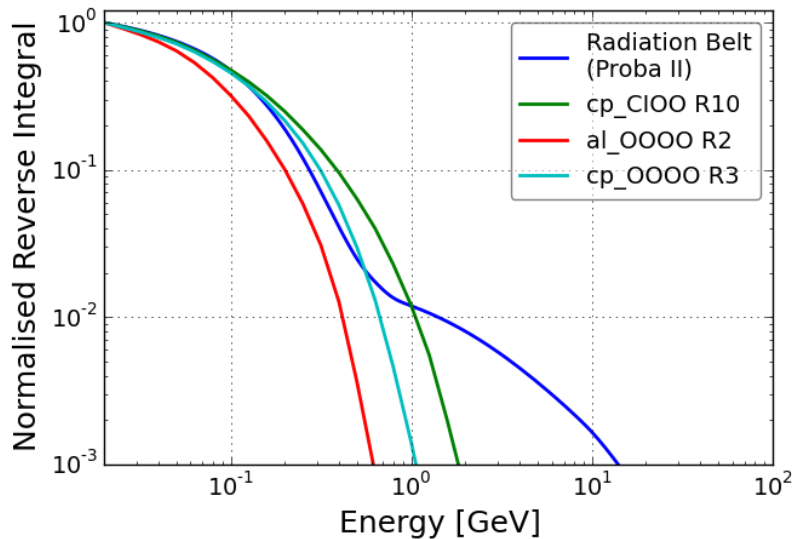


Figure 4.9: A plot of the reverse integral HEH spectrum for the proton belt (Proba II orbit), with a number of CHARM test configurations with close matches.

4.2 Copper Target without Shielding

The following results chapter focuses on the analysis of the calculations using the copper target configuration without shielding (`cp_OOOO`). The same tables and plots for the other facility configurations can be found in the appendix. All results tables can also be found at http://thornton.web.cern.ch/fluka_data.html

| Rack | Dose Gy/day | HEH /cm ² /day | Composition | | | | R | Hardness Energy | | |
|------|----------------|------------------------------|-------------|-------|-----------|------|------|-----------------|-------|-------|
| | | | n | p | π^\pm | k | | H50 | H10 | H1 |
| 1 | 1.65E+01 | 5.03E+10 | 82.90 | 7.04 | 9.54 | 0.20 | 3.48 | 0.06 | 0.18 | 0.38 |
| 2 | 1.81E+01 | 5.23E+10 | 82.50 | 7.08 | 9.80 | 0.23 | 3.15 | 0.06 | 0.19 | 0.41 |
| 3 | 3.41E+01 | 7.53E+10 | 72.40 | 13.00 | 14.00 | 0.44 | 2.05 | 0.09 | 0.31 | 0.69 |
| 4 | 3.43E+01 | 7.44E+10 | 70.30 | 13.70 | 15.30 | 0.49 | 2.06 | 0.10 | 0.36 | 0.78 |
| 5 | 3.16E+01 | 6.52E+10 | 69.80 | 13.80 | 15.70 | 0.57 | 2.37 | 0.11 | 0.41 | 0.89 |
| 6 | 3.46E+01 | 7.13E+10 | 66.40 | 15.60 | 17.10 | 0.62 | 2.19 | 0.12 | 0.47 | 0.99 |
| 7 | 3.39E+01 | 6.84E+10 | 64.90 | 16.10 | 18.10 | 0.70 | 2.30 | 0.13 | 0.51 | 1.12 |
| 8 | 3.23E+01 | 6.53E+10 | 63.20 | 16.70 | 19.20 | 0.74 | 2.39 | 0.14 | 0.58 | 1.23 |
| 9 | 3.10E+01 | 6.26E+10 | 62.30 | 16.80 | 19.90 | 0.83 | 2.51 | 0.15 | 0.63 | 1.38 |
| 10 | 3.61E+01 | 7.28E+10 | 58.80 | 17.20 | 22.70 | 1.11 | 2.05 | 0.19 | 0.78 | 1.67 |
| 11 | 8.04E+01 | 1.71E+11 | 34.50 | 23.50 | 37.70 | 4.06 | 0.74 | 1.79 | 6.84 | 12.60 |
| 12 | 1.57E+02 | 4.15E+11 | 24.50 | 49.10 | 23.60 | 2.60 | 0.30 | 7.01 | 23.00 | 24.00 |
| 13 | 6.77E+01 | 1.28E+11 | 41.30 | 19.50 | 35.60 | 3.41 | 1.03 | 0.73 | 3.35 | 6.51 |

Table 4.5: A table of the spectra content and hardness factors for the test area configuration with copper target and without shielding.

CHARM FLUKA Data Sets

Config: cp_OOOO
Normalisation: 1.5e+15

| rack | dose | heh | heheq | neu | thneq | silmev | r | dheh | h_1 | h_10 | h_50 | wff |
|------|----------|----------|----------|----------|----------|----------|-------|-------|--------|--------|-------|--------|
| - | Gy | /cm^2 | /cm^2 | /cm^2 | /cm^2 | /cm^2 | - | 1E-9 | GeV | GeV | GeV | - |
| 1 | 1.84E+01 | 3.29E+10 | 5.65E+10 | 9.39E+11 | 1.06E+11 | 4.49E+11 | 3.228 | 0.558 | 0.419 | 0.199 | 0.066 | 0.198 |
| 2 | 2.00E+01 | 3.56E+10 | 5.94E+10 | 9.31E+11 | 1.04E+11 | 4.43E+11 | 2.919 | 0.561 | 0.447 | 0.209 | 0.070 | 0.223 |
| 3 | 2.75E+01 | 4.65E+10 | 7.31E+10 | 9.70E+11 | 1.05E+11 | 4.89E+11 | 2.251 | 0.592 | 0.545 | 0.248 | 0.077 | 0.296 |
| 4 | 3.14E+01 | 5.13E+10 | 7.74E+10 | 9.70E+11 | 1.07E+11 | 4.85E+11 | 2.078 | 0.613 | 0.591 | 0.276 | 0.084 | 0.354 |
| 5 | 3.50E+01 | 5.57E+10 | 8.13E+10 | 9.61E+11 | 1.11E+11 | 4.74E+11 | 1.996 | 0.629 | 0.681 | 0.319 | 0.091 | 0.440 |
| 6 | 3.65E+01 | 6.01E+10 | 8.39E+10 | 9.40E+11 | 1.14E+11 | 4.53E+11 | 1.893 | 0.608 | 0.787 | 0.350 | 0.101 | 0.538 |
| 7 | 3.69E+01 | 6.13E+10 | 8.25E+10 | 9.04E+11 | 1.16E+11 | 4.18E+11 | 1.896 | 0.602 | 0.862 | 0.406 | 0.110 | 0.656 |
| 8 | 3.39E+01 | 5.46E+10 | 7.16E+10 | 8.42E+11 | 1.20E+11 | 3.54E+11 | 2.201 | 0.621 | 1.003 | 0.470 | 0.126 | 0.834 |
| 9 | 3.70E+01 | 6.05E+10 | 7.82E+10 | 8.36E+11 | 1.24E+11 | 3.58E+11 | 2.048 | 0.611 | 1.124 | 0.527 | 0.133 | 0.988 |
| 10 | 3.58E+01 | 5.86E+10 | 7.42E+10 | 8.00E+11 | 1.28E+11 | 3.26E+11 | 2.185 | 0.611 | 1.289 | 0.578 | 0.152 | 1.183 |
| 11 | 3.42E+01 | 5.71E+10 | 7.12E+10 | 7.67E+11 | 1.31E+11 | 3.01E+11 | 2.291 | 0.599 | 1.405 | 0.656 | 0.163 | 1.395 |
| 12 | 3.25E+01 | 5.47E+10 | 6.71E+10 | 7.36E+11 | 1.32E+11 | 2.75E+11 | 2.423 | 0.595 | 1.614 | 0.738 | 0.175 | 1.639 |
| 13 | 3.75E+01 | 6.53E+10 | 7.76E+10 | 7.42E+11 | 1.29E+11 | 2.80E+11 | 1.972 | 0.574 | 1.994 | 0.905 | 0.216 | 2.272 |
| 14 | 5.17E+01 | 9.10E+10 | 1.05E+11 | 7.82E+11 | 1.27E+11 | 3.23E+11 | 1.391 | 0.568 | 2.629 | 1.256 | 0.296 | 3.542 |
| 15 | 6.15E+01 | 1.14E+11 | 1.27E+11 | 7.97E+11 | 1.23E+11 | 3.37E+11 | 1.079 | 0.540 | 3.862 | 1.857 | 0.446 | 6.101 |
| 16 | 6.59E+01 | 1.24E+11 | 1.36E+11 | 7.96E+11 | 1.21E+11 | 3.31E+11 | 0.974 | 0.531 | 6.696 | 3.294 | 0.765 | 11.259 |
| 17 | 9.55E+01 | 2.13E+11 | 2.25E+11 | 8.21E+11 | 1.23E+11 | 3.71E+11 | 0.577 | 0.448 | 20.831 | 10.976 | 2.895 | 24.101 |
| 18 | 9.68E+01 | 2.01E+11 | 2.14E+11 | 8.37E+11 | 1.23E+11 | 3.82E+11 | 0.610 | 0.482 | 16.779 | 8.803 | 2.277 | 21.890 |
| 19 | 5.78E+01 | 1.02E+11 | 1.15E+11 | 8.26E+11 | 1.24E+11 | 3.30E+11 | 1.209 | 0.565 | 5.654 | 2.767 | 0.567 | 9.183 |

Operation successful!

Preliminary Data

Figure 4.10: An example of a data-table from the FLUKA calculations for the CHARM test positions.

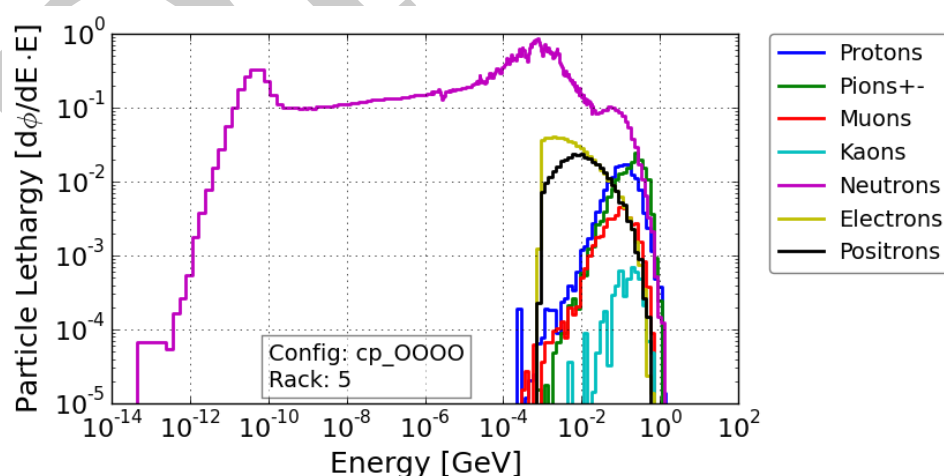


Figure 4.11: An example plot of the radiation spectra at a test position for the facility configuration with the copper target without shielding.

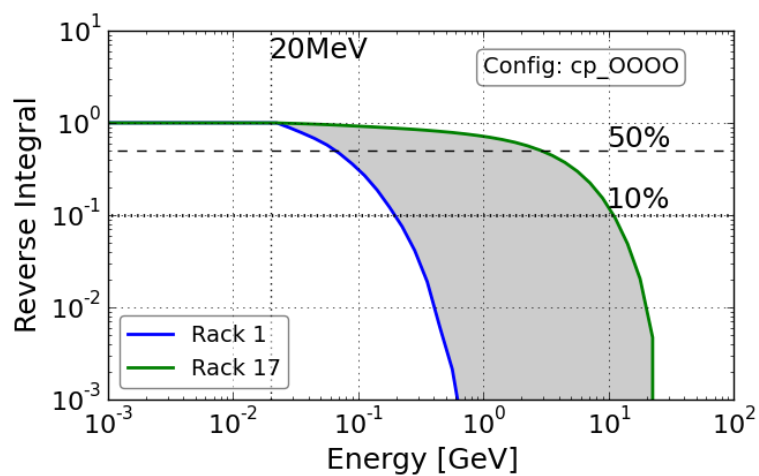


Figure 4.12: A plot of the reverse integral spectra for the case with the copper target without shielding.

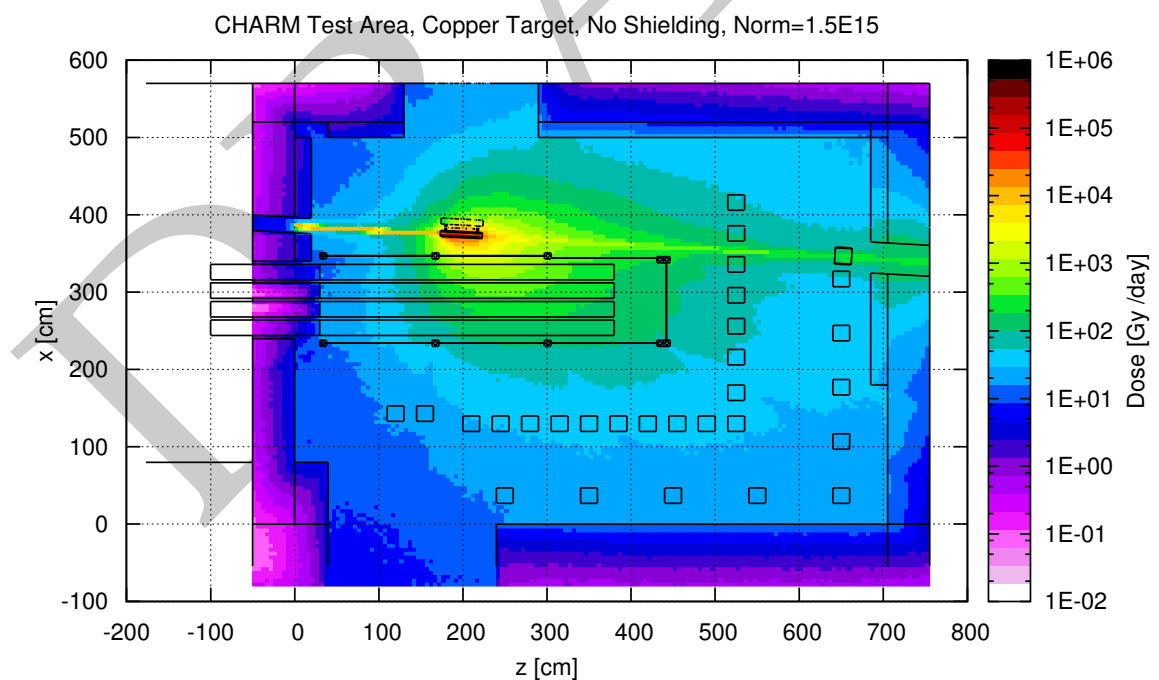


Figure 4.13: A plot of the dose per day inside the test area at beam height, normalised for the normal beam conditions.

4.3 Montrac Test Position

MAYBE BETTER IN THE INTRODUCTION

Testing at the Montrac location is typically performed without the target, which means the radiation field is dominated by the primary beam. Therefore it is only suitable for tests requiring a mono-energetic proton beam of 24 GeV. However as the dose rate and particle fluence is high, it is a good place for dose testing, radiation damage to materials, and for detector calibration purposes.

The test parameters are limited by the beam conditions, namely in the intensity and frequency of the spills, and the dimensions in the x and y plane. There are two main modes for the kind of beam sent to CHARM: target beam and blown-up beam conditions, shown in table X. These conditions can vary during operation, depending on the requirements for the various PS beam users.

Dose, HEH, 1MeV-eq n fluence in Si, beam size, gradients, peak values:

- In-beam tests (normal beam)
- In-beam tests (blown-up beam)
- Tests with target

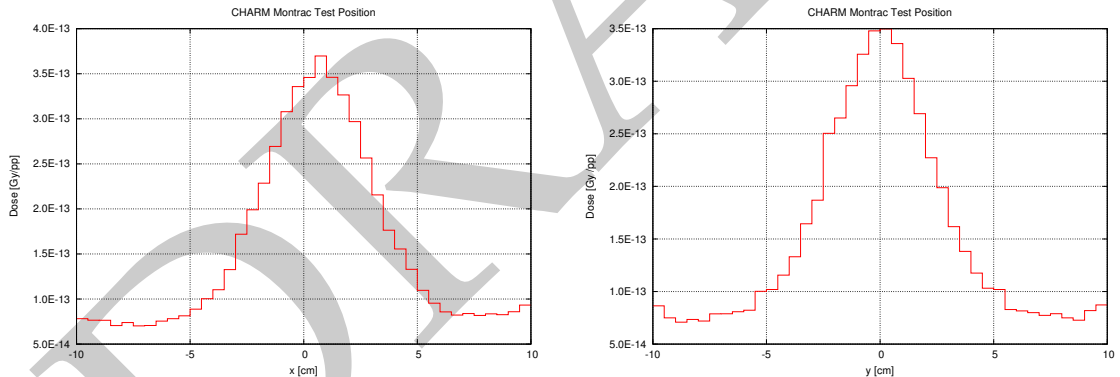


Figure 4.14: A plot of the dose profiles per proton at the Montrac test location (in beam).

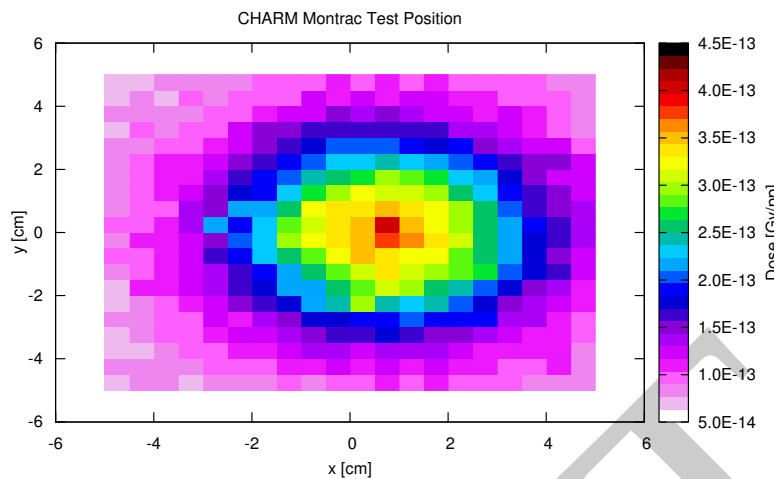


Figure 4.15: A plot of the dose per proton in 2D at the Montrac test location (in beam).

4.4 Uncertainties

There are a number of errors and uncertainties associated with the FLUKA calculations. The first main contributing factor is the accuracy of the geometry. This is in term of position of objects inside the main simulation geometry, materials and dimensions. Secondly there may be errors when comparing the calculations to tests made in the real facility due to positioning, and accurately the device was placed. There needs to be considerations for the test device itself, as the size of the sensitive volume may be large. These points are explored below with the aim of summarizing the various potential errors.

Gradients (in beam as well as test positions)

Chapter 5

Measurements and Testing

This chapter will summarise a number of measurements performed at CHARM, with the aim of later benchmarking the FLUKA calculated data, so that in the future we can rely confidently on the calculations, and minimise the number of measurements needed. There are a number of key areas of interest for the measurements which can be divided into the following; non-shielded test-area positions, shielded test-area positions, and the in-beam Montrac position.

5.1 Non-shielded Positions

5.2 Shielded Positions

5.3 BLM

5.4 Montrac

Chapter 6

Summary

Beep.

DRAFT

Appendix A

Facility Information

| Position | x [cm] | y [cm] | z [cm] |
|----------|--------|--------|--------|
| 1 | 143 | 129 | 120 |
| 2 | 143 | 129 | 155 |
| 3 | 130 | 129 | 210 |
| 4 | 130 | 129 | 245 |
| 5 | 130 | 129 | 280 |
| 6 | 130 | 129 | 315 |
| 7 | 130 | 129 | 350 |
| 8 | 130 | 129 | 385 |
| 9 | 130 | 129 | 420 |
| 10 | 130 | 129 | 455 |
| 11 | 130 | 129 | 490 |
| 12 | 130 | 129 | 525 |
| 13 | 170 | 129 | 525 |
| 14 | 215 | 129 | 525 |
| 15 | 255 | 129 | 525 |
| 16 | 295 | 129 | 525 |
| 17 | 335 | 129 | 525 |
| 18 | 375 | 129 | 525 |
| 19 | 415 | 129 | 525 |

Table A.1: A table of the test position coordinates in the CHARM test area, relative to the FLUKA geometry.

Appendix B

FLUKA Data

| Rack | HEH /cm ² / day | Composition | | | | R | Hardness Energy | | |
|------|----------------------------------|-------------|----|-----------|---|------|-----------------|-------|-------|
| | | n | p | π^\pm | k | | H50 | H10 | H1 |
| 1 | 1.70E+10 | 12 | 71 | 17 | 0 | 2.24 | 0.07 | 0.43 | 0.21 |
| 2 | 1.82E+10 | 11 | 70 | 17 | 0 | 2.00 | 0.08 | 0.47 | 0.22 |
| 3 | 2.26E+10 | 15 | 66 | 19 | 0 | 1.61 | 0.08 | 0.55 | 0.27 |
| 4 | 2.52E+10 | 16 | 64 | 20 | 0 | 1.47 | 0.09 | 0.62 | 0.29 |
| 5 | 2.77E+10 | 17 | 62 | 21 | 0 | 1.38 | 0.10 | 0.70 | 0.33 |
| 6 | 2.99E+10 | 18 | 60 | 21 | 0 | 1.31 | 0.11 | 0.80 | 0.38 |
| 7 | 3.10E+10 | 18 | 59 | 22 | 1 | 1.31 | 0.12 | 0.89 | 0.43 |
| 8 | 2.96E+10 | 18 | 58 | 23 | 1 | 1.43 | 0.13 | 1.05 | 0.50 |
| 9 | 3.33E+10 | 20 | 55 | 24 | 1 | 1.32 | 0.15 | 1.20 | 0.56 |
| 10 | 3.34E+10 | 20 | 54 | 25 | 1 | 1.36 | 0.17 | 1.33 | 0.64 |
| 11 | 3.38E+10 | 20 | 53 | 26 | 1 | 1.38 | 0.18 | 1.47 | 0.70 |
| 12 | 3.43E+10 | 20 | 52 | 27 | 1 | 1.39 | 0.19 | 1.67 | 0.79 |
| 13 | 4.17E+10 | 20 | 49 | 29 | 1 | 1.11 | 0.24 | 2.03 | 0.97 |
| 14 | 6.49E+10 | 21 | 43 | 35 | 2 | 0.70 | 0.35 | 2.74 | 1.35 |
| 15 | 9.32E+10 | 21 | 36 | 41 | 2 | 0.47 | 0.56 | 3.96 | 2.00 |
| 16 | 1.40E+11 | 20 | 30 | 47 | 3 | 0.30 | 1.06 | 6.85 | 3.54 |
| 17 | 4.36E+11 | 30 | 25 | 41 | 4 | 0.10 | 4.58 | 22.06 | 13.35 |
| 18 | 3.79E+11 | 27 | 25 | 45 | 4 | 0.11 | 3.61 | 18.12 | 10.72 |
| 19 | 1.22E+11 | 20 | 32 | 45 | 3 | 0.37 | 0.93 | 6.29 | 3.23 |

Table B.1: A table of the spectra content and hardness factors for the test area configuration with aluminium target and without shielding.

SEU Cross-section (σ_{seu})

The probability of causing a single event up-set in a memory, typically measured in units of $cm^2 bit^{-1}$

LET The linear energy transfer of a particle in a material, measured in $MeV cm^{-2} mg^{-1}$ **Critical-charge (Q_c)**

The charge required to cause an SEU (or SEE), measured in μC

Dose (D)

Energy deposited in a material due to radiation, measured in $\frac{J}{kg}$ in units Grays (Gy)

HEH Fluence (Φ_{HE})

The flux of high-energy hadron (hadrons over 20 MeV), per unit area and integrated over time, typically given in cm^{-2}

1 MeV Equivalent Neutron Fluence (in Silicon) (Φ_{1MeVn})

The equivalent fluence of 1 MeV neutrons that has the same damage effect (in Silicon), measured in cm^{-2}

Particle Fluence (Lethargy) ($\frac{d\Phi(E) \times E}{dE}$)

This is used in plots of particle fluence, where the fluence value has been multiplied by the energy binning width (often used in FLUKA), given in $cm^{-2} GeV^{-1}$

Table B.2: A table of useful definitions for various physical quantities [Thornton 2014]